AIP | Applied Physics Letters

Black silicon with controllable macropore array for enhanced photoelectrochemical performance

Xianyu Ao, Xili Tong, Dong Sik Kim, Lianbing Zhang, Mato Knez et al.

Citation: Appl. Phys. Lett. **101**, 111901 (2012); doi: 10.1063/1.4752231
View online: http://dx.doi.org/10.1063/1.4752231
View Table of Contents: http://apl.aip.org/resource/1/APPLAB/v101/i11
Published by the American Institute of Physics.

Additional information on Appl. Phys. Lett.

Journal Homepage: http://apl.aip.org/
Journal Information: http://apl.aip.org/about/about_the_journal
Top downloads: http://apl.aip.org/features/most_downloaded
Information for Authors: http://apl.aip.org/authors

ADVERTISEMENT

Downloaded 16 May 2013 to 158.227.184.199. This article is copyrighted as indicated in the abstract. Reuse of AIP content is subject to the terms at: http://apl.aip.org/about/rights_and_permissions

Black silicon with controllable macropore array for enhanced photoelectrochemical performance

Xianyu Ao,[1,2,a)] Xili Tong,[1] Dong Sik Kim,[1] Lianbing Zhang,[1] Mato Knez,[1,3] Frank Müller,[1] Sailing He,[4] and Volker Schmidt[1]

[1]*Max Planck Institute of Microstructure Physics, Weinberg 2, 06120 Halle, Germany*
[2]*Centre for Optical and Electromagnetic Research, South China Academy of Advanced Optoelectronics, South China Normal University, 510006 Guangzhou, China*
[3]*IKERBASQUE, Basque Foundation for Science, 48011 Bilbao, Spain and CIC nanoGUNE Consolider, 20018 Donostia-San Sebastian, Spain*
[4]*JORCEP [Joint Research Center of Photonics of the Royal Institute of Technology (Sweden), Zhejiang University and Lund University (Sweden)], Zijingang Campus, 310058 Hangzhou, China*

(Received 29 June 2012; accepted 29 August 2012; published online 10 September 2012)

Macroporous silicon with multiscale texture for reflection suppression and light trapping was achieved through a controllable electrochemical etching process. It was coated with TiO_2 by atomic layer deposition, and used as the photoanode in photocatalytic water splitting. A conformal pn-junction was also built-in in order to split water without external bias. A 45% enhancement in photocurrent density was observed after black silicon etching. In comparison with nano-structured silicon, the etching process here has neither metal contamination nor requirement of vacuum facilities. © *2012 American Institute of Physics*. [http://dx.doi.org/10.1063/1.4752231]

Black silicon is a surface modification of silicon wafer such that the reflectivity of visible (and infrared) light is extremely low, and many approaches have been developed to this end. Besides irradiating silicon with femtosecond laser pulses,[1] reactive ion etching[2,3] and metal-assisted wet etching[4–7] were previously employed to create random nano-spikes or nano-holes on silicon surface. The reflectivity is reduced by multiple reflection and absorption. These processes either involve vacuum facilities or introduce metal contamination.

In contrast to nano-structured silicon, macroporous silicon[8] has a much larger feature size, and established technologies to etch straight pores in silicon, with diameters in the range of sub-micrometers up to several micrometers as well as high aspect ratios, have been developed. Moreover, pores having large diameter variations on the length scale of the interpore distance can be achieved,[9–11] allowing the fabrication of complex three-dimensional (3D) structures like photonic crystals.[12] This 3D etching capability is unique among all the microfabrication techniques. Here we demonstrate that macroporous silicon can also be made black, and moreover, that light-trapping structures can be incorporated in a single run, by a simple and controllable electrochemical etching process.

The black macroporous silicon was obtained by exposing an anodically biased n-type ⟨100⟩ silicon wafer (bulk resistivity $\sim 5\ \Omega$ cm) to dilute hydrofluoric acid (5 wt. % HF at 10 °C). A hexagonal pattern of inverted pyramid-like pits on the exposed surface, defined by photolithography, served as the initial seeds for pore growth. The back side of the wafer was highly doped in order to easily make ohmic contacts. For a given interpore distance and fixed etching conditions, the pore diameter is determined by the current density flowing across the Si/HF interface, so that the diameter can be adjusted by tuning the current density via backside illumination.[8] By exerting a large current in the beginning and then decreasing the current gradually, a sharp blade-like structure was formed as shown in Fig. 1(a). The excess charge carriers spread over the pore wall, therefore, not only the pore bottom but also the wall was etched, leaving behind a tapered wall. After that, the diameter of the pores can be modulated[9,10] in order to realize the function of light trapping. Figure 1(b) shows the cross section of an array of 20 μm deep pores with two kinks obtained by this method. Our black silicon has multiscale texture, with nano-sized blades sitting on the top of micro-sized pore walls.

Reflectance measurement was taken with an integrating sphere (with a built-in tungsten-halogen light source) and two spectrometers (QE65000 and NIRQuest, Ocean Optics). As shown in Fig. 2(a), the total reflectance from our black silicon is below 5% over 400–1000 nm (the spectrum below 400 nm is not available due to the light source used for this measurement), and close to zero around 500 nm. Note that the interpore distance is much larger than the optical wavelength concerned so the periodicity does not matter.

We coated our black silicon with TiO_2 and used it as the photoanode in water splitting. In photocatalytic splitting of water into H_2 and O_2,[13,14] electrons and holes, generated in semiconductors upon light absorption, drive the reduction and oxidation reactions, respectively.

About 50 nm thick TiO_2 film was grown on silicon by atomic layer deposition (ALD)[15] in a commercial hot-wall flow-type ALD reactor (SUNALE R75, Picosun) at 300 °C with $TiCl_4$ and H_2O as precursors. The rough surface of the TiO_2 film, as shown in Fig. 1(c), indicates that the film is polycrystalline. The x-ray diffraction (XRD) characterization showed that the deposited TiO_2 has an anatase phase (band gap 3.2 eV). The photoelectrochemical (PEC) performance was evaluated in an air-tight Teflon cell with a quartz window using a potentiostat/galvanostat (Princeton Applied Research, 263 A). The electrolyte was 45 ml of 1 M KOH solution. The

[a)]Author to whom correspondence should be addressed. Electronic mail: xao@mpi-halle.mpg.de.

 © 2012 American Institute of Physics

Downloaded 16 May 2013 to 158.227.184.199. This article is copyrighted as indicated in the abstract. Reuse of AIP content is subject to the terms at: http://apl.aip.org/about/rights_and_permissions

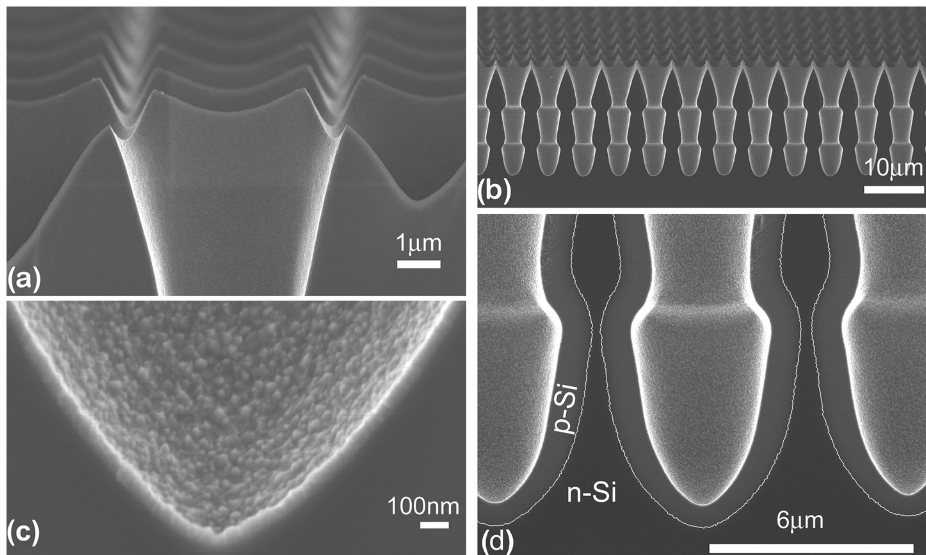

FIG. 1. Cross-sectional SEM images of black macroporous silicon. The pores were arranged in a hexagonal pattern with an interpore distance of 6 μm. (a) Tilted top view of the entrance of the etched pores, showing the sharp blade-like structures. (b) Tilted view of the modulated pore array (20 μm deep; the dark part is silicon) coated with TiO_2 by ALD at 300 °C. (c) Magnified view of the bottom of one pore, showing the rough surface of the TiO_2 film. (d) Cross-sectional SEM image (taken at 3.0 kV) showing the conformal p-n junction in macroporous silicon. The separation of p- and n-type regions is highlighted via a white curve. From the contrast, the thickness of the p-type layer is estimated to be around 700 nm.

reference electrode was Ag/AgCl in 3 M KCl, and a Pt coil was used as the counter electrode. The irradiation was from a Xe lamp (svx 1000, Mueller-Elektronik), and a fan-cooled KG-2 filter (2 mm, Schott) was used to avoid solution heating by infrared light. Conductive silver paste was used to contact the back side of silicon, and the working electrode was 7 cm away from the quartz window. The light intensity at the position of the working electrode (without electrolyte) was about 85 mW/cm^2. The illuminated area of the working electrode has a diameter of 1.5 cm. The scan rate for the linear sweep voltammetry was 10 mV/s. The electrolyte was continuously bubbled with argon to remove the dissolved oxygen. As a control, samples prior to electrochemical etching, taken from the same starting wafer (with inverted pyramid-like pits, see Fig. 2(b)), were also measured.

Gray lines of Fig. 3(a) shows typical plots of the photocurrent density versus the bias potential against the Ag/AgCl reference electrode (*J–V* curves) for two kinds of working electrodes, i.e., black n-Si and the control sample (both coated with TiO_2). The dark current density of the control sample is around 2 μA/cm^2, and that of our black silicon is approximately twofold. Figure 3(a) (gray lines) indicates that, under illumination, TiO_2 coated black n-Si has about

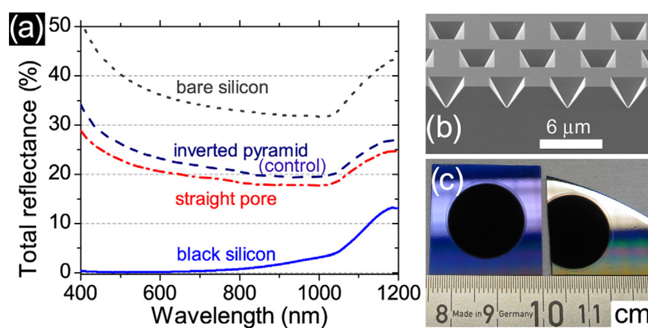

FIG. 2. Measured total reflectance spectra (a) from silicon with inverted pyramid-like pits (with an opening size of 3 μm × 3 μm, see (b) for its bird's eye view under SEM; dashed line), straight pores (diameter 3 μm and depth 20 μm; dashed-dotted line), and the present black silicon (solid line; see also (c) for its digital photograph under room light: the circular etched area appears black; the left one has 50 nm TiO_2 coating, while the right one has not). As a reference, the reflectance from bare silicon is also shown (dotted line). All samples for this reflection measurement have no TiO_2 coating.

40% higher photocurrent density and a slightly more negative onset potential as compared with the control sample. The photocurrent density and onset potential are comparable to those from n-TiO_2 coated n-Si nanowire arrays reported in the literature.[16,17] Increasing the surface area of photoelectrodes can reduce the overpotential for gas evolution[7] (therein nano-structured p-type black silicon was used as a photocathode to produce H_2 from water, and a 20% enhancement relative to a polished sample was observed). The relative shift of the onset potential after black silicon etching is not as dramatic as the case with silicon nanowire array,[16] which reflects that the relative increase of surface area in our case is much smaller (this point should be beneficial for photovoltaic applications which means relatively low surface recombination rate in comparison with nano-structured silicon). For water splitting applications, the surface area can be further increased by etching deeper pores with smaller interpore distance and pore diameter.

To understand the contribution arising from the surface structures, we also measured samples with straight pores of similar depth (diameter 3 μm and depth 20 μm; one may find what a straight pore looks like in Fig. 2 of Ref. 18). Texturing the silicon surface can reduce the total reflection and correspondingly enhance the light absorption and also increase the surface area. However, increased surface area also means higher surface recombination loss. The macroporous silicon with straight pores has a much larger surface area and slightly lower total reflectance (see Fig. 2(a)) than our control sample (the silicon with inverted pyramid-like pits), however, PEC measurements on a TiO_2 coated straight-pore sample showed only slightly higher photocurrent density (within 5% as compared to the control sample). This is quite different from the significant enhancement of photocurrent density with our black silicon, i.e., about 40%. We therefore attribute the great enhancement in photocurrent of TiO_2 coated black macroporous silicon to that the increase in the optical absorption (for both TiO_2 and silicon) heavily outweighs the increase in the surface recombination loss. Although both kinds of macroporous structures can trap weakly absorbed photons to some extent, only the black one can achieve broad band reflection suppression and absorption

Downloaded 16 May 2013 to 158.227.184.199. This article is copyrighted as indicated in the abstract. Reuse of AIP content is subject to the terms at: http://apl.aip.org/about/rights_and_permissions

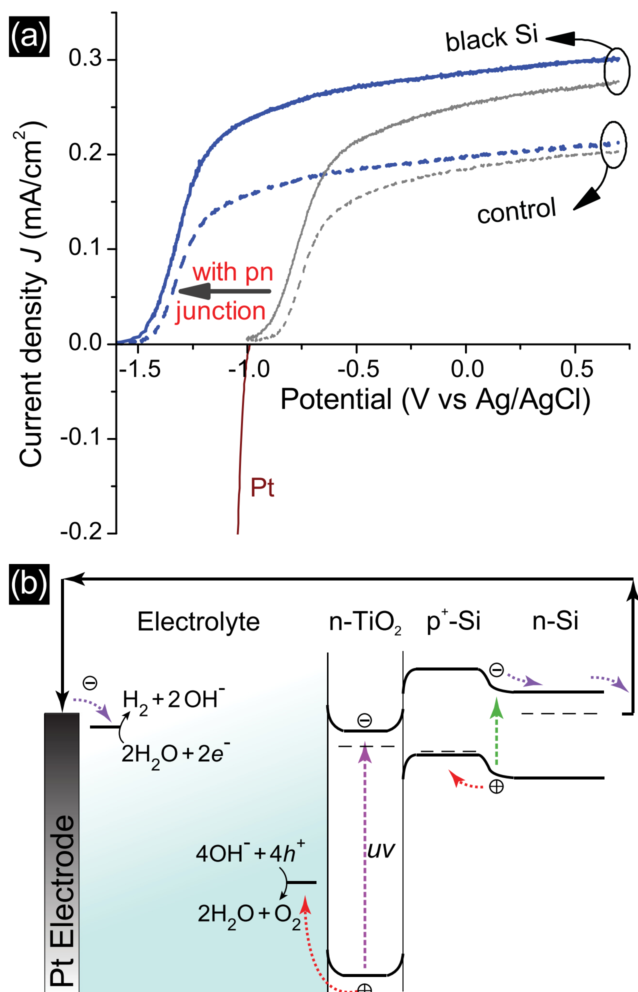

FIG. 3. (a) Measured photocurrent density as the bias potential (vs Ag/AgCl) varies for the case of TiO_2 coated n-Si (gray lines) or TiO_2 coated pn-Si (blue lines) in 1 M KOH electrolyte, showing the enhanced photocurrent after black silicon etching (solid lines) in comparison with the control sample (with inverted pyramid-like pits; dashed lines). The shift of the onset potential by the built-in photovoltaic cell is about −0.55 V. For reference, the *J–V* curve for hydrogen evolution at the Pt electrode is also shown (dark red). (b) Schematic band diagram for water splitting with Pt–TiO_2/pn-Si under illumination.

enhancement, in which the nano-sized sharp blade-like structures are helpful to couple short wavelength light into semiconductors, while the micro-sized modulated pores can further scatter long wavelength light.

The onset potential for TiO_2/n-Si photoanodes is around −1 V (vs Ag/AgCl), close to the normal hydrogen evolution at the Pt electrode (see Fig. 3(a)). A pn-junction can be incorporated before deposition of TiO_2, and the photovoltage from the illuminated junction can shift the onset potential to the negative side, in such a way that photoelectrolysis by a Pt–TiO_2/pn-Si pair can occur spontaneously.[19] Here a conformal pn-junction was realized, for both the black silicon sample and the control sample, by a high-temperature diffusion procedure (950 °C for 40 min) using spin-on dopant (B154, Filmtronics) on the front side as boron source and a thermally grown 200 nm thick oxide layer on the back side as the diffusion barrier. Our macroporous silicon is quite robust, and the black feature will not disappear after thermal oxidation. The thickness of the p-type layer is estimated to be around 700 nm from the contrast of the SEM image[20] (see Fig. 1(d)). Such a conformal pn-junction is analogous to the radial one formed on silicon wires[21–29] and is believed to have a short distance for minority charge carrier collection. The measured *J–V* curves of TiO_2 coated pn-Si are shown in Fig. 3(a) as blue lines. The dark current density with pn-junction is smaller than the case without pn-junction. The onset potential is shifted by about −0.55 V by the built-in photovoltaic cell, which absorbed the irradiation not absorbed yet by TiO_2. Upon illumination, electron-hole pairs are generated in both TiO_2 and Si. By shorting the TiO_2/pn-Si electrode and the Pt counter electrode, water can be split directly with light. As schematically shown in Fig. 3(b), the photo-generated holes in TiO_2 are transferred to the TiO_2/electrolyte interface to oxidize OH^-, while photo-generated electrons in the silicon pn-junction (directed to the Pt counter electrode through the external circuit) have sufficient cathodic potential for water reduction. To complete the circuit, holes from silicon and electrons from TiO_2 recombine at the Si/TiO_2 interface. Measurement of the photocurrent by shorting TiO_2/pn-Si and Pt confirmed that current is flowing from Pt to Si in the external circuit. Our results show that the black silicon etching process can improve the photocurrent density by 45%. By comparing the curves for the control samples with and without pn-junction, we see that the introduction of a pn-junction did not bring any unfavorable potential barrier. The additional enhancement, 45% for the case with pn-junction while 40% for the case without pn-junction, may be due to better surface passivation, since the oxidation during the preparation of pn-junctions can create atomically flat silicon surface.

In summary, we have demonstrated that black silicon with a modulated macropore array can achieve significant light absorption enhancement. In the multiscale texture, the nano-sized sharp blade-like structures and the micro-sized modulated pores are helpful for coupling short wavelength light and scattering long wavelength light, respectively. We observed a 45% enhancement in photocurrent density in photocatalytic water splitting by the present black pn-silicon coated with TiO_2, in comparison with the control sample (TiO_2 coated pn-silicon with inverted pyramid-like pits). In contrast to black silicon structured by other methods, the etching process reported here has neither metal contamination nor requirement of vacuum facilities. Furthermore, our black silicon is quite robust for fabrication processes like high-temperature thermal oxidation.

X.A. wishes to thank K. Sklarek and the mechanical workshop staff for their assistance, Dr. S. Senz for fruitful discussions, Dr. A. Chopra for XRD measurement, and Dr. Jinwei Gao and Mr. Qinhui Hu for reflection measurement. Partial support from NSFC (61204074) is acknowledged.

[1]T.-H. Her, R. J. Finlay, C. Wu, S. Deliwala, and E. Mazur, Appl. Phys. Lett. **73**, 1673 (1998).
[2]M. Otto, M. Kroll, T. Käsebier, S.-M. Lee, M. Putkonen, R. Salzer, P. T. Miclea, and R. B. Wehrspohn, Adv. Mater. **22**, 5035 (2010).
[3]L. Sainiemi, V. Jokinen, A. Shah, M. Shpak, S. Aura, P. Suvanto, and S. Franssila, Adv. Mater. **23**, 122 (2011).
[4]S. Koynov, M. S. Brandt, and M. Stutzmann, Appl. Phys. Lett. **88**, 203107 (2006).
[5]H. M. Branz, V. E. Yost, S. Ward, K. M. Jones, B. To, and P. Stradins, Appl. Phys. Lett. **94**, 231121 (2009).

Downloaded 16 May 2013 to 158.227.184.199. This article is copyrighted as indicated in the abstract. Reuse of AIP content is subject to the terms at: http://apl.aip.org/about/rights_and_permissions

[6]F. Toor, H. M. Branz, M. R. Page, K. M. Jones, and H.-C. Yuan, Appl. Phys. Lett. **99**, 103501 (2011).
[7]J. Oh, T. G. Deutsch, H.-C. Yuan, and H. M. Branz, Energy Environ. Sci. **4**, 1690 (2011).
[8]V. Lehmann, *Electrochemistry of Silicon: Instrumentation, Science, Materials and Applications* (Wiley, Weinheim, 2002).
[9]F. Müller, A. Birner, J. Schilling, U. Gösele, C. Kettner, and P. Hänggi, Phys. Status Solidi A **182**, 585 (2000).
[10]S. Matthias, F. Müller, J. Schilling, and U. Gösele, Appl. Phys. A **80**, 1391 (2005).
[11]A. Langner, M. Knez, F. Müller, and U. Gösele, Appl. Phys. A **93**, 399 (2008).
[12]S. Matthias, F. Müller, C. Jamois, R. B. Wehrspohn, and U. Gösele, Adv. Matter. **16**, 2166 (2004).
[13]A. Fujishima and K. Honda, Nature **238**, 37 (1972).
[14]M. G. Walter, E. L. Warren, J. R. McKone, S. W. Boettcher, Q. Mi, E. A. Santori, and N. S. Lewis, Chem. Rev. **110**, 6446 (2010).
[15]M. Knez, K. Nielsch, and L. Niinistö, Adv. Mater. **19**, 3425 (2007).
[16]Y. J. Hwang, A. Boukai, and P. D. Yang, Nano Lett. **9**, 410 (2009).
[17]J. Shi, Y. Hara, C. Sun, M. A. Anderson, and X. Wang, Nano Lett. **11**, 3413 (2011).
[18]S. Matthias, F. Müller, and U. Gösele, Appl. Phys. Lett. **87**, 224106 (2005).
[19]H. Morisaki, T. Watanabe, M. Iwase, and K. Yazawa, Appl. Phys. Lett. **29**, 338 (1976).
[20]M. EI-Gomati, F. Zaggout, H. Jayacody, S. Tear, and K. Wilson, Surf. Interface Anal. **37**, 901 (2005).
[21]B. Tian, X. Zheng, T. J. Kempa, Y. Fang, N. Yu, G. Yu, J. Huang, and C. M. Lieber, Nature **449**, 885 (2007).
[22]J. R. Maiolo, B. M. Kayes, M. A. Filler, M. C. Putnam, M. D. Kelzenberg, H. A. Atwater, and N. S. Lewis, J. Am. Chem. Soc. **129**, 12346 (2007).
[23]E. C. Garnett and P. D. Yang, J. Am. Chem. Soc. **130**, 9224 (2008).
[24]E. C. Garnett and P. D. Yang, Nano Lett. **10**, 1082 (2010).
[25]M. D. Kelzenberg, S. W. Boettcher, J. A. Petykiewicz, D. B. Turner-Evans, M. C. Putnam, E. L. Warren, J. M. Spurgeon, R. M. Briggs, N. S. Lewis, and H. A. Atwater, Nature Mater. **9**, 239 (2010).
[26]S. W. Boettcher, E. L. Warren, M. C. Putnam, E. A. Santori, D. Turner-Evans, M. D. Kelzenberg, M. G. Walter, J. R. McKone, B. S. Brunschwig, H. A. Atwater, and N. S. Lewis, J. Am. Chem. Soc. **133**, 1216 (2011).
[27]S. W. Boettcher, J. M. Spurgeon, M. C. Putnam, E. L. Warren, D. B. Turner-Evans, M. D. Kelzenberg, J. R. Maiolo, H. A. Atwater, and N. S. Lewis, Science **327**, 185 (2010).
[28]M. D. Kelzenberg, D. B. Turner-Evans, M. C. Putnam, S. W. Boettcher, R. M. Briggs, J. Y. Baek, N. S. Lewis, and H. A. Atwater, Energy Environ. Sci. **4**, 866 (2011).
[29]T. J. Kempa, J. F. Cahoon, S.-K. Kim, R. W. Day, D. C. Bell, H.-G. Park, and C. M. Lieber, Proc. Natl. Acad. Sci. U.S.A. **109**, 1407 (2012).

Downloaded 16 May 2013 to 158.227.184.199. This article is copyrighted as indicated in the abstract. Reuse of AIP content is subject to the terms at: http://apl.aip.org/about/rights_and_permissions